Journal of Applied Polymer Science

Urea-activated 4,4′-oxibis-(benzenesulfonyl hydrazide) as foaming agent for low-density unsaturated polyester resin manufacturing

Yi-Fan Zhang, Xiao-Jun Wang, Zhi-Gang Pan, Cheng-Ming Hong, Gao-Feng Ji
Department of Composite Materials, College of Materials Science and Engineering, Nanjing Tech University, Nanjing 210009, People's Republic of China
Correspondence to: X.-J. Wang (E-mail: xjwang@njtech.edu.cn)

ABSTRACT: The activation of foaming agent is critical to its application. In this study, 4,4′-oxibis-(benzenesulfonyl hydrazide) (OBSH) activated by urea was used in the manufacture of low-density unsaturated polyester resin (LDUPR), and the results were compared with that of OBSH activated by zinc oxide and zinc stearate. The experiment results showed that the activation of OBSH by urea was better than by zinc oxide or by zinc stearate. A novel hydrogen bond activation mechanism of urea is presented in this research. Two stages, including the induction stage and the foaming stage, were proposed in the LDUPR manufacture according to the gas evolution curves of activated OBSH. The decomposition temperature and the decomposition time of OBSH activated by urea were determined to match the gelation time of UPR for the manufacture of LDUPR. The disadvantageous chemical behaviors of activated OBSH were eliminated in the induction treatment. The activated OBSH via induction treatment released gas maximally and distributed gas homogeneously in the resin glue, resulting in a better foaming effect than that of the previous foaming agents. © 2015 Wiley Periodicals, Inc. J. Appl. Polym. Sci. **2015**, *132*, 42824.

KEYWORDS: foams; manufacturing; resins; thermosets

Received 27 October 2014; accepted 9 August 2015
DOI: 10.1002/app.42824

INTRODUCTION

Unsaturated polyester resin (UPR) and its products are widely used in various areas, such as automotive industry, construction, electronic industry, and so on. In recent years, low-density unsaturated polyester resin (LDUPR) with its unique properties and broad application prospects has received much attention and become the focus of material research and manufacture.[1–5] Foaming is the most widely used technique for the LDUPR manufacture than light-weight filler padding.

Foaming technology includes physical foaming and chemical foaming. Chlorofluorocarbon and hydrofluorocarbon are the commercial foaming agents used in physical foaming process. However, they are outlawed in many countries because of the damage to the ozone layer and the greenhouse effect.[6,7] Chemical foaming is appreciated as the most potential method, which is studied and used extensively at present. Especially, organic chemical foaming agents play important roles in the manufacture of light-weight organic thermosetting resin, such as LDUPR. Azodicarbonamide (AC), azodiisobutyronitrile (AIBN) of the azo class, and 4,4′-oxibis-(benzenesulfonyl hydrazide) (OBSH) of the sulfonyl hydrazide class are the most commercial ones among organic chemical foaming agents.[8] Guo *et al.*[4] reported a dual-initiation and dual-foaming mechanism based on a composite foaming agent containing AIBN and azobisisoheptonitrile (ABVN) and prepared LDUPR. Such work made a new progress in the LDUPR manufacture, but the toxicity of azo limits the application of azo foaming agents.

The nontoxic foaming agent OBSH decomposes exothermically and releases nitrogen, water and nonpolar oligomers in its foaming process.[9] The heat released from the decomposition of the hydrazine portion was partially compensated for by the energy consumed in the reduction of the sulfonyl group, and the overall heating was thus quite moderate.[10] In addition, OBSH is nonstaining and nondiscoloring, which can meet the product's demand of pure color. However, there is no report related to the production of LDUPR with the presence of OBSH. It is because OBSH decomposes from 140°C to 160°C resulting in the rapid cure of UPR that goes against the growth of homogeneous porous structure. Therefore, activation should be carried out for OBSH to match the molding conditions for LDUPR manufacture.

In previous research, zinc oxide and zinc stearate were used as activators to modify azo class, and thermal analysis was applied to discuss the change of decomposition temperature.[11–16] Using base, such as urea or amine, to activate OBSH is a well-known

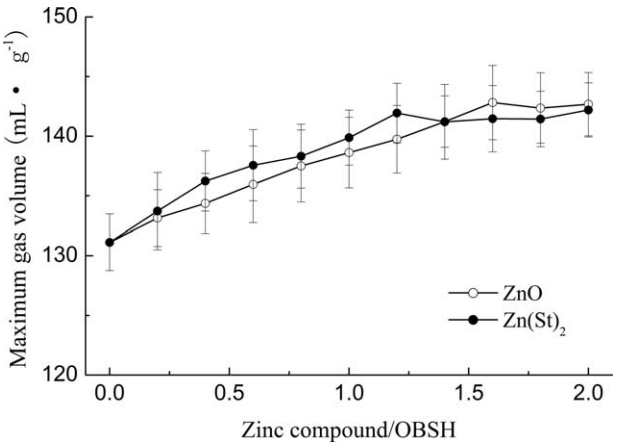

Figure 1. The maximum gas volume of activated OBSH with different contents of zinc compound.

technique.[9,17–19] Therefore, this study aimed to investigate the utilization of urea compared with zinc compounds as OBSH activators, and study the activation mechanism. In this study, differential scanning calorimetry (DSC) was used to determine the change of decomposition temperature with the addition of activators. Besides the curing temperature, the homogenous resin/gas glue is critical to foaming, and the decomposition time of foaming agents should match the gelation time of resin glue.[20–22] Therefore, according to the gas evolution curves of activated OBSH, the decomposition process of activated OBSH was divided into two stages, i.e., the induction stage and the foaming stage. In the induction stage, the disadvantageous chemical behaviors of activated OBSH could be eliminated via preheating; then in the foaming stage, the activated OBSH could decompose rapidly in resin glue to foam UPR effectively.

The research aimed to investigate the activation of OBSH by urea. A novel activation mechanism of urea acting on OBSH was proposed in the manuscript, and was confirmed by DSC, variable-temperature Fourier transform infrared (FTIR) spectroscopy, and variable-concentration nuclear magnetic resonance (NMR) analysis.

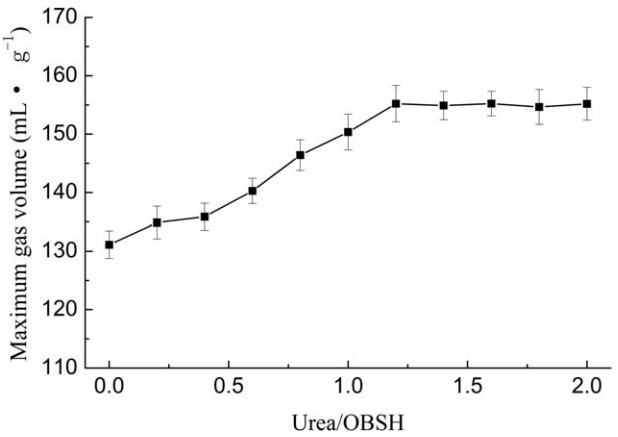

Figure 2. The maximum gas volume of activated OBSH with different contents of urea.

EXPERIMENTAL

Materials

The UPR used in this work was an orthophthalic polyester resin obtained from Jinling DSM Resins Co., China. OBSH and *p*-toluenesulfonyl hydrazide (TSH) were produced by Shanghai Darui Fine Chemical Co., China. The initiator used in this work was a commercial product from Akzo Nobel N.V containing more than 98 wt % tert butylperoxy benzoate (TBPB). The activators used in this study were urea (99 wt %), zinc oxide (99 wt %), and zinc stearate (99 wt %) produced by Xilong Chemical Co., China. The secondary and tertiary amines used in the experiment were dimethyl urea (98 wt %) produced by Adames Reagent Co., and tetramethyl urea (99 wt %) produced by Aladdin Industrial Corp., China.

Measurement of the Gas Volume

The maximum gas volume of foaming agent was measured by a volumetric gas-burette experiment.[23–25] The foaming agent was heated from room temperature to 160°C ± 2°C at the heating rate of 5°C min^{-1}.

The gas evolution curve of activated OBSH at a certain temperature was also measured by the gas-burette experiment. The temperature was set at 110, 115, 120, 125, and 130°C, respectively. The controlling precision of temperature is less than ±0.1°C.

Preparation of the Specimens

The activated OBSH was prepared by grinding the mixed powder of OBSH and activator, including urea, zinc oxide, and zinc stearate. The mass ratio of activator to OBSH was set from 0.2 to 2.0 at an interval of 0.2 in the experiment to study the effect of the addition of activator on OBSH.

During the induction treatment, which was suggested in the experiment of induction stage of activated OBSH, an appropriate amount of activated OBSH powder was added into the mould. The proper preheated temperature range was obtained from Table VII, and the treatment time was calculated from the

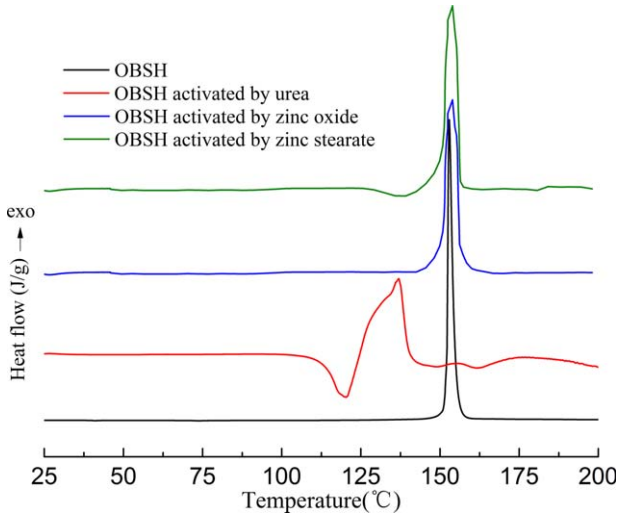

Figure 3. The DSC thermograms of OBSH and activated OBSH. [Color figure can be viewed in the online issue, which is available at wileyonlinelibrary.com.]

Table I. The Specific Heat Capacity of OBSH, $Zn(St)_2$, and ZnO at Different Temperatures

Specific heat capacity ($J\ g^{-1}\ K^{-1}$)	Temperature (°C)						
	50	55	60	65	70	75	80
OBSH	0.17	0.18	0.18	0.19	0.19	0.20	0.20
$Zn(St)_2$	0.45	0.45	0.47	0.48	0.48	0.49	0.50
ZnO	0.49	0.51	0.51	0.52	0.53	0.54	0.55

equation obtained from Figure 10. After the treatment, the resin glue with the initiator in a specific ratio was added into the mould and stirred uniformly for the LDUPR manufacture.

The LDUPR specimens were prepared according to a formula of 100 g resin, 1 g initiator, and 1 g activated OBSH to determine the optimal molding temperature of the LDUPR. The molding temperature was varied from 115°C to 125°C with an interval of 2.5°C.

To investigate the appropriate content of activated OBSH, the LDUPR specimens were prepared according to a formula with a mass ratio of 100 g resin to 1 g initiator, and the content of activated OBSH was varied from 1 to 3 wt % of resin with an interval of 0.5 wt %. All the LDUPR specimens were cured for 1 h at molding temperature of 115.0, 117.5, 120.0, 122.5, and 125°C. Finally, the specimens were cooled down to room temperature.

Property Testing

The gel time of UPR was measured with a gel time meter (GT-2, Lin'an Fengyuan Electronics Co., China). The apparent density was detected according to ISO 845-2006. The compression strength and tensile strength of the specimens were measured with an electronic universal testing machine (WDW3100, Changchun Xinke Instrument Co., China, maximum pressure = 100 kN and accuracy = 0.5%), according to ISO 844:2014 (Rigid Cellular Plastics—Determination of Compression Properties) and ISO 1926:2009 (Rigid Cellular Plastics—Determination of Tensile Properties) at the ambient temperature of 23°C ± 2°C and a relative humidity of 50% ± 5%. In a parallel experiment, five replicated specimens were tested for each formula, and the experiment was repeatable.

Differential Scanning Calorimetry (DSC)

NETZSCH DSC204 differential scanning calorimeter was used for measuring the exothermic heat of pure OBSH and OBSH activated by urea. The specimens were sealed in a volatile aluminum sample pan. Nonisothermal scans were carried out from 25°C to 200°C at a heating rate of 10°C min^{-1} under the nitrogen atmosphere. The modulation of temperature for DSC was ±0.1°C. The mass of foaming agent specimens in the experiment was 3∼7 mg, and the sensitivity of the DSC was 0.1 μg.

Fourier Transform Infrared (FTIR) Spectroscopy

The effect of activators on OBSH was characterized by an FTIR spectrometer (Nicolet Nexus 670) with a resolution of 2 cm^{-1}. Pressed KBr discs were used. Thirty-two scans from 4000 to 400 cm^{-1} were taken for each specimen. The spectra were baseline-corrected.

^{1}H Nuclear Magnetic Resonance (^{1}H NMR)

The (^{1}H NMR) spectrum was obtained by a Bruker AVANCE 400 MHz (9.37T) NMR equipped with 5 mm BBO probe for the analysis of the decomposition residues of activated OBSH. The samples were dissolved in DMSO. To obtain spectra, we used the standard pulse sequence with a delay time of 1 s. The spectra were registered after 32 scans. Chemical shifts are referenced to the resonance of TMS.

Analysis of Morphology

The sections of the specimens were observed by an adjustable auto-fine-tune portable microscope (A005$^+$, Shenzhen D&F Co., China) to investigate the micro morphology of the samples.

RESULTS AND DISCUSSION

Effect of Zinc Oxide and Zinc Stearate on the Activation of OBSH

The relation between the zinc compound addition and the maximum gas volume of activated OBSH is shown in Figure 1. As for pure OBSH, the maximum gas volume is 131.1 ± 1.4 mL g^{-1}. It is deduced from Figure 1 that the addition of zinc compound lowered the decomposition temperature and promoted the decomposition process.

Combining with Figure 1, it reveals that the activation became more significant with the increase of the content of zinc compound activator and OBSH decomposed easily with the maximum gas volume slightly increase. The maximum gas volume of activated OBSH became stable after the addition of zinc compound activators was beyond a certain value, whereas the decomposition of OBSH accomplished.

When the mass ratio of zinc oxide to OBSH was 1.6, the maximum gas volume of activated OBSH reached the maximum value of 142.8 ± 3.1 mL g^{-1}. As of the mass ratio of zinc

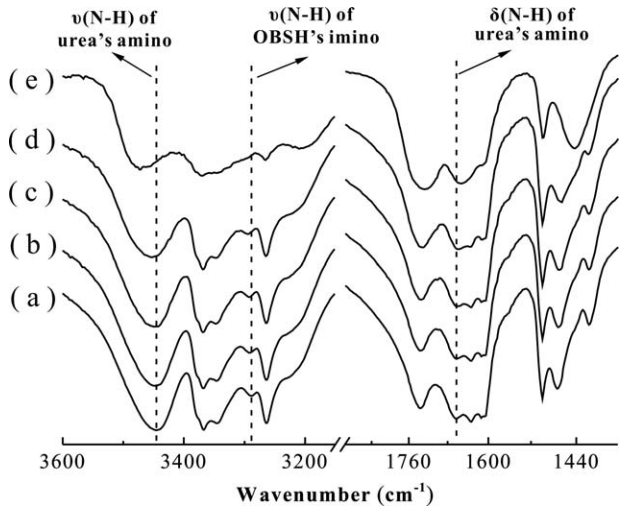

Figure 4. Variable-temperature FTIR spectra of OBSH/urea at (a) 15, (b) 75, (c) 95, (d) 113, and (e) 125°C.

Table II. Offsets of Infrared Characteristic Peaks for the Hydrogen Bond Related Groups

Assignments of OBSH/ urea mixture	Wavenumber (cm^{-1})					Offsets (cm^{-1})
	15°C	75°C	95°C	115°C	125°C	
υ(N—H) of urea's amino group	3445.6	3446.3	3448.3	3452.9	3472.2	+26.6
δ(N—H) of urea's amino group	1624.3	1623.8	1623.6	1620.6	1616.3	−8.0
υ(N—H) of OBSH's imino group	3288.6	3291.6	3292.0	3294.1	3318.1	+29.5

stearate to OBSH being 1.2, the maximum gas volume of activated OBSH was 141.9 ± 2.5 mL g^{-1}. The activation of the two zinc compound activators was similar.

Effect of Urea on the Activation of OBSH

The relation between the urea addition and the maximum gas volume of activated OBSH is shown in Figure 2. In this figure, when the mass ratio of urea to OBSH is no less than 1.2, the maximum gas volume of activated OBSH becomes a stable value of 155.2 ± 3.1 mL g^{-1}.

The change of decomposition temperature and exotherm heat of pure OBSH and activated OBSH were explored by DSC experiment. The DSC thermogram is shown in Figure 3. It shows that the exothermic peak of pure OBSH is at 151.92°C and the exothermic heat is 381.5 J g^{-1}. With the presence of urea, the exothermic peak of OBSH/urea sample changes to 135.87°C, and the exothermic heat of OBSH/urea is 169.4 J g^{-1}. The endothermic peak appearing before the exothermic peak of OBSH/urea is corresponding to the fusion of urea,[26] which resulted in the decrease of the overall exothermic heat of the OBSH/urea system.

In addition, the exothermic peak of OBSH/zinc oxide and OBSH/zinc stearate is at 153.83°C and 152.65°C respectively, and the exothermic heat is 276.3 and 251.2 J g^{-1}, respectively. The exothermic peak temperatures of OBSH/zinc oxide and OBSH/zinc stearate are slightly higher than the exothermic peak temperatures of pure OBSH (at 151.92°C). It is attributed to the competitive heat absorption of zinc compound and OBSH in the mixture. Zinc compound took the advantage of bigger specific heat capacity (Table I), leading to the hysteresis of the OBSH/zinc compound exothermic peak. (The specific heat capacity was measured according to ISO 11357-4:2005 standard *Plastics-Differential Scanning Calorimetry (DSC)-Part 4: Determination of Specific Heat Capacity*, and the results are listed in Table I.)

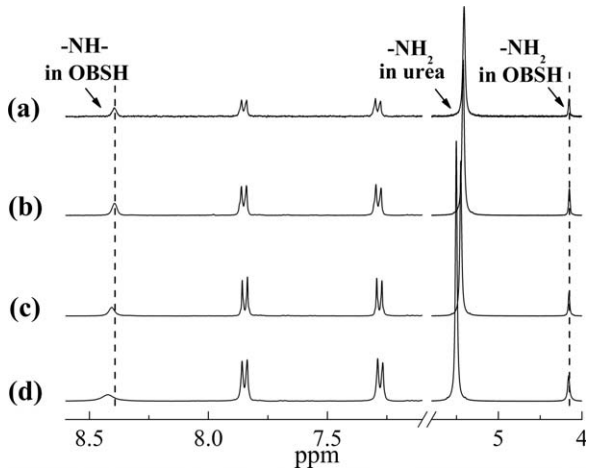

Figure 5. Partial proton NMR spectra of OBSH/urea at various concentrations: (a) 15.52, (b) 155.25, (c) 310.49, and (d) 776.24 m*M*.

Zinc compounds exhibited weaker activation and higher exothermic heat compared with urea. Therefore, urea is the optimal activator for OBSH in the LDUPR manufacture.

It was deduced that the activation by urea is due to the hydrogen bond based on the experiment earlier. The hydrogen bonds are formed between the hydrogen atoms in urea and the nitrogen atom of imino group in OBSH. With the presence of hydrogen bond, charge transfer occurred from the nitrogen atom (the acceptor) to the nitrogen–hydrogen group (the donor), which weakened the nitrogen–sulfur bond, making it easier to break down. Consequently, the hydrogen bonding between urea and OBSH resulted in the activation of OBSH. Moreover, the molten state of urea appeared around 110°C, and also provided a favorable condition for the formation of hydrogen bond.

Hydrogen Bond Activation Mechanism

According to Refs. 27−33, variable-temperature FTIR and variable-concentration ^{1}H NMR were used to verify the hydrogen bond.

Variable-Temperature FTIR. Previous researches[27–30] indicated that, on the premise of the existence of hydrogen bonds, as temperature rises, the hydrogen bond becomes weaker, stretching vibration of corresponding groups shift to higher wavenumber, whereas the bending vibration of corresponding groups shift to lower wavenumber. These changes can be characterized by variable-temperature infrared experiment.

The variable-temperature FTIR spectra of OBSH/urea mixture at 15, 75, 95, 115, and 125°C are shown in Figure 4. The offsets of infrared characteristic peaks for the hydrogen bond related groups are listed in Table II.

Table II indicates that, with the temperature rising from 15°C to 125°C, the stretching vibrations of urea's amino group (υ(N-H) = 3445.6 cm^{-1}) and OBSH's imino group (υ(N-H) = 3288.6 cm^{-1}) in OBSH/urea mixture shift to higher wavenumber by 26.6 and 29.5 cm^{-1}, respectively, whereas the bending vibration of urea's amino group (δ(N-H) = 1624.3 cm^{-1}) shifts to lower wavenumber by 8.0 cm^{-1}. These changes were consistent with the rules that as the temperature rises, the hydrogen bond becomes weaker.[28–30] Variable-temperature FTIR illustrated that

Table III. ^{1}H Chemical Shifts for Corresponding Groups at Various Concentrations

Assignment of OBSH/ urea mixture	Chemical shift (ppm)				
	15.52 m*M*	155.25 m*M*	310.49 m*M*	776.24 m*M*	Offset (ppm)
—NH— in OBSH	8.383	8.389	8.402	8.426	0.043
—NH_2 in urea	5.401	5.416	5.446	5.505	0.104
—NH_2 in OBSH	4.154	4.151	4.153	4.152	-

hydrogen bond was formed between OBSH's imino group and urea's amino group.

Variable-Concentration NMR. According to the discussion of hydrogen bond in Ref. 27, the hydrogen bond led to characteristic NMR signals that typically include pronounced proton deshielding for H, through hydrogen bond spin–spin couplings and nuclear Overhauser enhancements.[27] In this case, the chemical shift of proton downfield shift. In the solution NMR, as the solution concentration increases, the hydrogen bond becomes stronger in the solution and leads to the effect of the proton deshielding enhancing. As a result, the chemical shift biases to downfield state.[29–33]

Therefore, the variable-concentration ^{1}H NMR experiment was carried out with the OBSH/urea mixture's concentration of 15.52, 155.25, 310.49, and 776.24 m*M* in DMSO. The partial ^{1}H NMR spectra of OBSH/urea mixture at various concentrations are shown in Figure 5. The chemical shifts and assignments at various concentrations are listed in Table III.

Table III indicates that with the increase of the OBSH/urea mixture concentration in DMSO from 15.52 to 776.24 m*M*, both imino group of OBSH ($\delta = 8.426$ ppm) and amino group of urea ($\delta = 5.505$ ppm) downfield shifted with the offsets of 0.043 ppm and 0.104 ppm, respectively. However, the chemical shift of OBSH's amino ($\delta = 4.152$ ppm) is stable with the increase of the concentration in Table III.

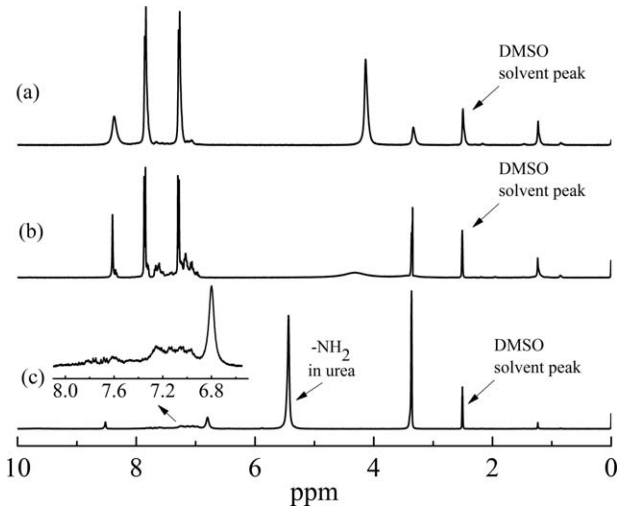

Figure 6. ^{1}H NMR spectra of (a) OBSH, (b) residue of OBSH at 150°C, and (c) residue of activated OBSH at 110°C.

These changes agreed with the rules described in Refs. 29−33. The hydrogen bond between imino group of OBSH and amino group of urea was reconfirmed by variable-concentration ^{1}H NMR. There is no hydrogen bond between the terminal amino group of OBSH and urea due to no chemical shift changing.

^{1}H NMR for the Residue of Activated OBSH. The ^{1}H NMR spectra for the residue of activated OBSH and the residue of OBSH at different temperatures are shown in Figure 6. The chemical shift and assignment of ^{1}H NMR spectra are listed in Table IV. The decomposition reaction of OBSH has two steps.[34] First, OBSH decomposed into sulfenic acid (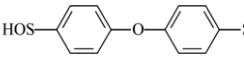), nitrogen, and water. After that, a disproportionation took place, and polymeric disulfide (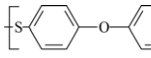) and thiosulfate (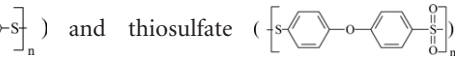) were generated. Two residues, which were polymeric disulfide and thiosulfate, remained during the two-step reaction process. Figure 6 shows that the decomposition of OBSH at 150°C ± 0.1°C was incomplete and undecomposed OBSH (the chemical shifts are 7.845 ppm and 7.300 ppm) remained in the residues. On the other hand, with the presence of urea, OBSH decomposed thoroughly at a lower temperature of 110°C. The ^{1}H NMR spectra apparently proved the existence of polymeric disulfide (the chemical shift is 6.799 ppm) and thiosulfate (the chemical shifts are ranging from 6.965 to 7.277 ppm) at 110°C ± 0.1°C. Furthermore, it was deduced that the urea had not decomposed during the decomposition process of OBSH (the chemical shift is 5.435 ppm), and urea just lower the decomposition temperature of OBSH via the formation of hydrogen bond.

Table IV. Experimental ^{1}H NMR Chemical Shift and Assignment

Specimen	Chemical shift, δ (ppm)	Assignment
OBSH	4.138	—NH_2
	7.858, 7.268	 in OBSH
	8.374	—NH—
Residue of OBSH at 150°C	4.316	—NH_2
	7.845, 7.300	 in OBSH
	8.392	—NH—
Residue of activated OBSH at 110°C	6.799	 in polymeric disulfide
	6.965-7.277	 in thiosulfate

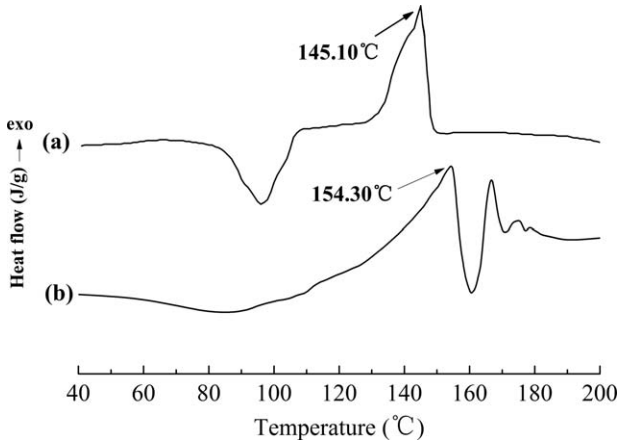

Figure 7. The DSC thermograms of (a) OBSH/dimethyl urea mixture and (b) OBSH/tetramethyl urea mixture.

In summary, the hydrogen bond produced by urea presented a novel activation mechanism for the foaming agent OBSH. The hydrogen bond weakened the covalent bond and accelerated the decomposition of foaming agents, resulting in the reduction of decomposition temperature.

Effect of Secondary and Tertiary Amines on OBSH

Dimethyl urea and tetramethyl urea are set as the secondary and tertiary amines to verify the earlier hydrogen bonding activation mechanism on the OBSH.

DSC Analysis. The DSC curves of OBSH/dimethyl urea mixture and OBSH/tetramethyl urea mixture are shown in Figure 7. Figure 7 shows that the exothermic peaks of OBSH/dimethyl urea and OBSH/tetramethyl urea are at 145.10°C and 154.30°C, respectively. Compared with the exothermic peak temperature of pure OBSH (at 151.92°C), the exothermic peak temperature of OBSH has a reduction of 6°C with the presence of dimethyl urea. However, the exothermic peak of OBSH/dimethyl urea is still higher than that of OBSH/urea mixture (at 135.87°C). The exothermic peak temperature of OBSH/tetramethyl urea does not reduce compared with the exothermic peak temperature of pure OBSH.

DSC analysis indicates that dimethyl urea has activation on OBSH. The activation of OBSH by dimethyl urea is weaker than that by urea. However, there was no activation effect generated between tetramethyl urea and OBSH.

Variable-Concentration NMR. In the DMSO solution, the molar ratios of OBSH/dimethyl and OBSH/tetramethyl urea were maintained at 0.14 (i.e., the mass ratio of dimethyl urea to OBSH being 1.76 and the mass ratio of tetramethyl urea to OBSH being 2.32), to have a parallel comparison with that of variable-concentration NMR experiment of OBSH/urea earlier (Figure 5). The chemical shifts and assignments for corresponding groups of OBSH/dimethyl urea and OBSH/tetramethyl urea at various concentrations are listed in Table V.

Table V indicates that for the OBSH/dimethyl urea, both imino group of OBSH and imino group of dimethyl urea downfield shift with the offsets of 0.016 ppm and 0.034 ppm respectively, which is less than those of imino group of OBSH and amino group of urea in OBSH/urea variable-concentration NMR experiment (0.043 ppm and 0.104 ppm). The earlier experiment indicated that hydrogen bond was formed between the secondary amine of dimethyl urea and the imino group of OBSH. Moreover, the hydrogen bond between dimethyl urea and OBSH showed a smaller binding stability compared with that between urea and OBSH due to the smaller chemical shifts,[31,32] which led to the weaker activation of dimethyl urea on OBSH compared with that of urea.

On the other hand, no hydrogen bond was identified between tetramethyl urea and OBSH, because the four methyl groups combine with the nitrogen atoms of tetramethyl urea. As a result, tetramethyl urea has no activation on OBSH.

Effect of Urea on TSH

Such activation of hydrogen bonding on the sulfonyl hydrazide foaming agents was reconfirmed in the decomposition of TSH. TSH, in a pure state, decomposed at 110°C ± 0.4°C, and the maximum gas volume of TSH was measured to be 117.8 ± 2.4 mL g^{-1}. The relation between the urea addition and the maximum gas volume of activated TSH is shown in Figure 8. As of the mass ratio of urea to TSH being 1.0, the maximum gas volume of activated OBSH reached to a stable value of 134.1 ± 3.1 mL g^{-1}.

Therefore, according to the experiment results earlier, urea was set as the optimal activator among the activators in the experiment. The decomposition temperature of activated OBSH was lower than the curing temperature of the UPR, fulfilling the demand of LDUPR manufacture. In the following experiment, the decomposition time of activated OBSH was adjusted to match the gel time of the UPR.

Induction Stage of Activated OBSH in the LDUPR Manufacturing

In the experiment, the treatment temperatures of activated OBSH were set at 110°C, 120°C, and 130°C to make activated OBSH decompose according to the DSC curves of activated

Table V. ^{1}H Chemical Shifts for Corresponding Groups of OBSH/Dimethyl Urea and OBSH/Tetramethyl Urea at Various Concentrations

		Chemical shift (ppm)			
Specimen	Assignment	155.25 mM	310.49 mM	776.24 mM	Offsets (ppm)
OBSH/dimethyl urea mixture	—NH— in OBSH	8.389	8.390	8.405	0.016
	—NH— in dimethyl urea	5.724	5.730	5.758	0.034
OBSH/tetramethyl urea mixture	—NH— in OBSH	8.395	8.398	8.400	0.005
	CH_3 in tetramethyl urea	2.692	2.694	2.696	0.004

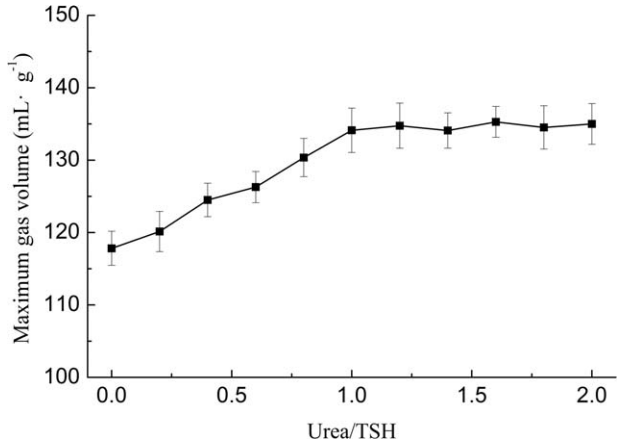

Figure 8. The maximum gas volume of activated TSH with different contents of urea.

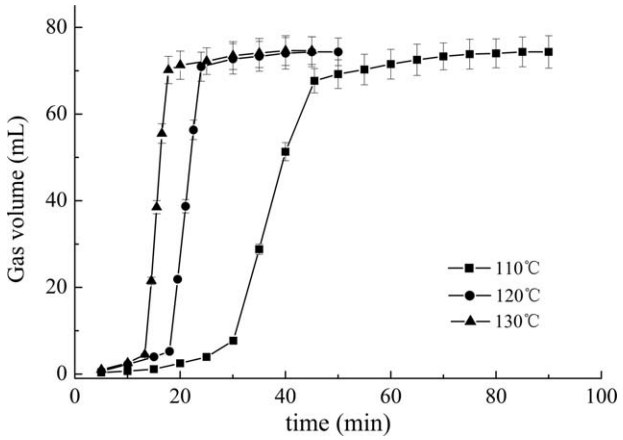

Figure 9. The gas evolution curves of activated OBSH at different temperatures.

OBSH. Figure 9 shows the gas evolution curves of activated OBSH at different temperatures.

Figure 9 illustrates that, at the early stage, the activated OBSH processed a small gas evolution and a slow decomposition speed. After a certain time, the decomposition rate of activated OBSH began to accelerate and the gas evolution increased rapidly. Lastly, the gas evolution curves of activated OBSH became gentle.

Based on the gas evolution change earlier, the decomposition process of activated OBSH was divided into three stages in the experiment, which were the induction stage of a small gas evolution and a slow decomposition rate at the beginning of decomposition; the foaming stage of a great gas evolution and a rapid decomposition rate by the middle of the decomposition; and the offgas stage of a little gas evolution at the end of the decomposition. The offgas stage was ignored in the work because of the tiny amount of gas released. The time of the induction stage and the foaming stage, marked as t_i and t_f, respectively, coincide with the two essential stages.

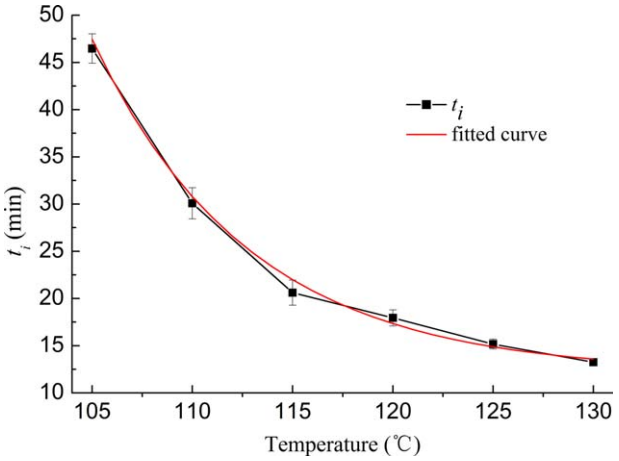

Figure 10. The nonlinear fitting of the change of t_i with the treatment temperature. [Color figure can be viewed in the online issue, which is available at wileyonlinelibrary.com.]

For bringing out the relation between the t_i of activated OBSH and treatment temperature, the experiment of the gas evolution curves of activated OBSH at 115°C and 125°C were done and the t_i at 110, 115, 120, 125, and 130°C are summarized in Table VI. Table VI indicates that the t_i decreases with the rise of the treatment temperature, and the change of t_i becomes relatively flatter over 120°C. A nonlinear fitting was carried out to establish a formula between the change of the t_i and the treatment temperature as shown in Figure 10.

Calculation shows that the change of the t_i with the treatment temperature satisfies the eq. (1), where T represents the treatment temperature and t_i represents the induction time.

$$t_i = 1.136^{(-T+132.957)} + 12.126 \quad (1)$$

The t_i of activated OBSH at a T temperature can be calculated by the equation. The t_i value calculated by the formula was accurate to the second decimal place to match the commercial manufacture of LDUPR.

Considering the slow decomposition rate and little gas evolution at the induction stage of activated OBSH, the induction treatment was proposed in which activated OBSH was preheated to pass through the induction stage of a small gas evolution and a slow decomposition rate. After the induction treatment,

Table VI. The t_i of Activated OBSH at Different Temperatures

	Temperature (°C)					
	105	110	115	120	125	130
t_i (min)	46.5 ± 2.2	30.1 ± 1.6	20.6 ± 1.4	18.0 ± 0.8	15.2 ± 0.5	13.2 ± 0.4

Table VII. The t_f of Activated OBSH and the Gel Time of UPR with 1 g Initiator per 100 g UPR at Different Temperatures

	Temperature (°C)					
	105	110	115	120	125	130
t_f (min)	30.2 ± 1.2	15.4 ± 0.8	9.1 ± 0.4	6.0 ± 0.3	5.0 ± 0.1	4.4 ± 0.1
Gel time with 1% tert buty lperoxy benzoate (min)	16.2 ± 0.8	12.8 ± 0.6	8.8 ± 0.4	6.5 ± 0.3	5.1 ± 0.1	3.8 ± 0.1

activated OBSH entered the foaming stage of a great gas evolution and a rapid decomposition rate, adapting to the manufacture of LDUPR. The t_i at various temperatures of the induction treatment could be obtained from eq. (1).

Different from AIBN and ABVN, the decompositions of most foaming agents, such as AC or activated OBSH, were not first-order reactions. It meant that most foaming agents could not decompose rapidly at the beginning of the decomposition, and various chemical behaviors exhibited before the adequately decomposition of the foaming agents, which led to inefficient foaming process. However, based on the discussion earlier, the adverse chemical behaviors could be eliminated in the induction treatment, and made the decomposition of foaming agents enter the foaming stage directly and foaming agents decompose rapidly during the manufacture of LDUPR. The idea of induction treatment improved the foaming process and extended the area of foaming agent application.

Foaming Stage of Activated OBSH in the LDUPR Manufacturing

The t_f of activated OBSH and the gel time of UPR with 1g initiator per 100g UPR at different temperatures are summarized in Table VII. The homogeneous gas/resin glue could form when the gel time of resin glue matched the t_f of activated OBSH. Therefore, five specific temperatures, 115.0, 117.5, 120.0, 122.5, and 125.0°C, were set in the experiment according to the data in Table VII.

As for the determination of the optimal molding temperature of the LDUPR, the t_i of the induction treatment was computed by eq. (1). The LDUPR specimens were prepared according to the formula of 100g resin : 1g initiator : 1g foaming agent. The properties of the LDUPR specimens cured at molding temperature of 115.0, 117.5, 120.0, 122.5, and 125°C are detected and listed in Table VIII compared with those of the specimens cured at 110.0°C and 130.0°C.

Table VIII. The Properties of LDUPR with 1 g Activated OBSH at Different Temperatures

Molding temperature (°C)	t_i (min)	Apparent density (g cm^{-3})	Compressive strength (10% deformation) (MPa)	Specific compressive strength (MPa g^{-1} cm^3)	Tensile strength (MPa)	Specific tensile strength (MPa g^{-1} cm^3)
110.0	30.8	0.82 ± 0.03	20.52 ± 0.69	24.82 ± 1.13	8.18 ± 0.35	9.55 ± 0.45
115.0	22.0	0.54 ± 0.02	12.35 ± 0.43	22.96 ± 1.02	3.60 ± 0.11	6.83 ± 0.33
117.5	19.3	0.41 ± 0.01	13.99 ± 0.51	33.84 ± 1.31	4.38 ± 0.13	10.23 ± 0.30
120.0	17.3	0.42 ± 0.01	13.63 ± 0.48	32.25 ± 1.29	4.10 ± 0.12	9.52 ± 0.31
122.5	15.9	0.40 ± 0.02	12.72 ± 0.44	30.61 ± 1.15	3.83 ± 0.13	9.27 ± 0.35
125.0	14.9	0.40 ± 0.01	12.56 ± 0.41	30.22 ± 1.22	3.22 ± 0.13	8.26 ± 0.35
130.0	13.6	0.84 ± 0.02	18.26 ± 0.54	22.13 ± 1.01	7.14 ± 0.29	8.80 ± 0.33

Table IX. The Properties of LDUPR with Different Contents of Activated OBSH

Content of the foaming agent (g/100 g of resin)	Apparent density (g cm^{-3})	Compressive strength (10% deformation) (MPa)	Specific compressive strength (MPa g^{-1} cm^3)	Tensile strength (MPa)	Specific tensile strength (MPa g^{-1} cm^3)
1.0	0.41 ± 0.01	13.99 ± 0.51	33.84 ± 1.31	4.38 ± 0.13	10.23 ± 0.30
1.5	0.41 ± 0.02	13.81 ± 0.52	33.59 ± 1.42	4.21 ± 0.11	9.98 ± 0.28
2.0	0.39 ± 0.01	13.76 ± 0.47	34.71 ± 1.53	4.18 ± 0.12	10.55 ± 0.31
2.5	0.38 ± 0.01	13.73 ± 0.48	35.72 ± 1.37	4.20 ± 0.10	11.21 ± 0.35
3.0	0.39 ± 0.02	13.22 ± 0.51	33.96 ± 1.42	3.87 ± 0.10	9.82 ± 0.29

Table X. The Properties of LDUPR with 2.5 g Activated OBSH at Different Temperatures

Molding temperature (°C)	t_i (min)	Apparent density (g cm^{-3})	Compressive strength (10% deformation) (MPa)	Specific compressive strength (MPa g^{-1} cm^3)	Tensile strength (MPa)	Specific tensile strength (MPa g^{-1} cm^3)
110.0	30.8	0.80 ± 0.02	19.72 ± 0.66	24.75 ± 1.11	7.70 ± 0.21	9.02 ± 0.38
115.0	22.0	0.52 ± 0.02	12.03 ± 0.46	22.57 ± 1.05	3.56 ± 0.15	6.95 ± 0.27
117.5	19.3	0.38 ± 0.01	13.73 ± 0.48	35.72 ± 1.37	4.20 ± 0.10	11.21 ± 0.35
120.0	17.3	0.40 ± 0.01	12.95 ± 0.43	32.55 ± 1.34	3.62 ± 0.13	9.18 ± 0.34
130.0	13.6	0.81 ± 0.02	18.36 ± 0.64	21.77 ± 0.99	7.29 ± 0.25	8.26 ± 0.33

Table XI. The Properties of LDUPR with Activated OBSH, Activated OBSH via Induction Treatment, and AIBN/ABVN Composite Foaming Agent

Foaming agent	Apparent density (g cm^{-3})	Compressive strength (10% deformation) (MPa)	Specific compressive strength (MPa g^{-1} cm^3)
Activated OBSH without induction treatment	0.65 ± 0.02	13.04 ± 0.43	20.10 ± 0.95
Activated OBSH with induction treatment	0.38 ± 0.01	13.73 ± 0.48	35.72 ± 1.37
AIBN/ABVN [4]	0.37 ± 0.01	12.99 ± 0.45	35.58 ± 1.63

Table VIII shows that the density of specimen stabilized around 0.40 g cm^{-3} at the temperature ranging from 117.5°C to 125°C, which was significantly lower than that at 110°C and 130°C. It was because that the t_f of activated OBSH was similar to the gel time of UPR from 117.5°C to 125°C (see Table VII), which provided enough time for the gas to dissolve in the resin glue and prevented the bubbles from escaping from the resin glue. At 110°C and 130°C, the t_f of activated OBSH was greater than the gel time of UPR. In this case, activated OBSH did not decompose completely before the gelation of UPR, leading to the large density of specimen.

In the temperature range of 117.5°C–125°C, the compressive strength and tensile strength of the specimen decreases with the increase of the temperature, owing to the decomposition rate of foaming agent and the gelation of resin both accelerating as the temperature rising. It is attributed to the rapid curing process of the UPR, resulting in a heterogeneous bubble distribution inside the specimen with the compressive strength and tensile strength decrease. The LDUPR specimen presented an apparent density of 0.41 ± 0.01 g cm^{-3}, an optimal specific compressive strength of 33.84 ± 1.31 MPa g^{-1} cm^3, and an optimal specific tensile strength of 10.23 ± 0.30 MPa g^{-1} cm^3, while the addition of activated OBSH being 1 wt % of the UPR, the temperature at 117.5°C, and the t_i being 19.3 min.

The content of the foaming agent was also an important factor to the properties of LDUPR. Based on the earlier experiment, the effect of the content of activated OBSH on the properties of LDUPR were studied when the molding temperature was at 117.5°C and the t_i was 19.3 min. In practice, the addition of a foaming agent is usually lower than 3.0 wt % of the resin,[35] hence, the addition of activated OBSH was set from 1.0 to 3.0 wt % of UPR at 0.5 wt % intervals. The experiment results are

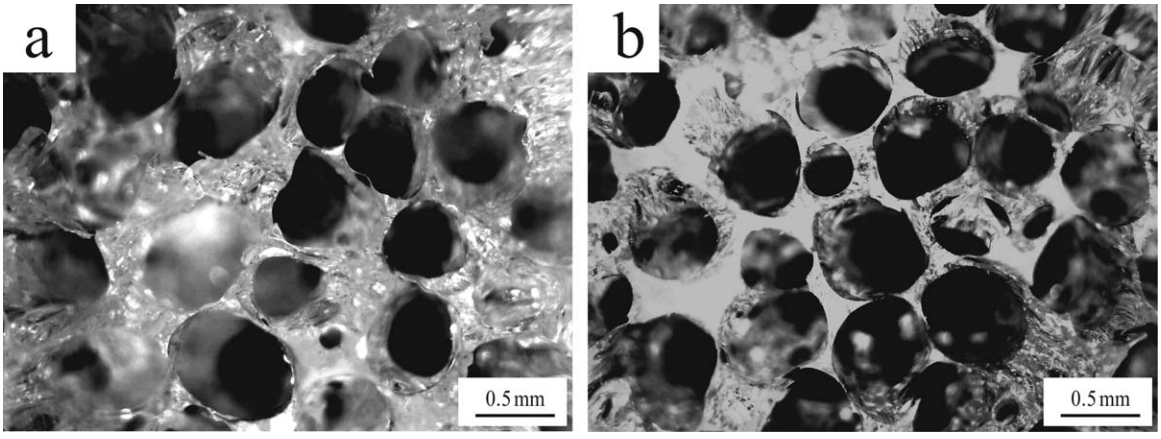

Figure 11. The micrographs of LDUPR with (a) activated OBSH and (b) activated OBSH via induction treatment.

listed in Table IX. Table IX shows that the optimal addition of activated OBSH was 2.5 wt % of the UPR, corresponding to the apparent density of 0.38 ± 0.01 g cm^{-3}, the specific compressive strength of 35.72 ± 1.37 MPa g^{-1} cm^3, and the specific tensile strength of 10.55 ± 0.31 MPa g^{-1} cm^3. Consequently, the addition of activated OBSH being 2.5 wt % of the UPR, the temperature at 117.5°C and the t_i being 19.3 min were set as the optimal conditions for the LDUPR manufacture.

The properties of LDUPR with 2.5 grams activated OBSH at temperatures ranging from 110°C to 130°C are listed in Table X. Table X shows that at the optimal molding temperature (117.5°C) obtained from Table VIII, the LDUPR specimen with 2.5g activated OBSH shows the optimal properties (apparent density of 0.38 ± 0.01 g cm^{-3}, specific compressive strength of 35.72 ± 1.37 MPa g^{-1} cm^3, and the specific tensile strength of 10.55 ± 0.31 MPa g^{-1} cm^3). It reconfirmed that the optimal molding temperature was at 117.5°C, while the addition of activated OBSH was 2.5g per 100g UPR.

In the manufacture of LDUPR, it is expected that the properties of LDUPR could be close to those of commercial rigid polyurethane foams (apparent density of 0.3∼0.4 g cm^{-3}, compressive strength of 10∼14 MPa g^{-1} cm^3, and tensile strength of 2.1∼2.4 MPa g^{-1} cm^3).[36] The properties of LDUPR specimen obtained via the preparation method in the work reached the desired properties. It reveals the feasibility and the universality of the preparation method proposed in the work.

The properties of the LDUPR specimens, which contained the activated OBSH, the activated OBSH via induction treatment, and the AIBN/ABVN composite foaming agent, are listed in Table XI. It is revealed that the properties of LDUPR prepared via induction treatment, similar to the properties of LDUPR prepared via AIBN/ABVN composite foaming agent,[4] was superior to that of LDUPR without induction treatment.

The micrographs of LDUPR specimens are shown in Figure 11. The figure illustrates that the porous structure of LDUPR with activated OBSH via induction treatment was more homogeneous than that of LDUPR with activated OBSH merely, which reconfirmed the superiority of induction treatment.

CONCLUSIONS

The OBSH activated by urea adapted to the LDUPR manufacture. With the presence of urea, the exothermic peak temperature and the exothermic heat of activated OBSH were reduced. As of the mass ratio of urea/OBSH being 1.2, the exothermic peak temperature of activated OBSH decreased to 135.87°C and the exothermic heat reduced to 169.4 J g^{-1}. A novel activation mechanism of urea, i.e., the formation of hydrogen bond between urea and OBSH, was proposed in the study. The activation mechanism was confirmed by the characterization of DSC, FTIR and NMR.

During the preparation of LDUPR, the decomposition process of activated OBSH was divided into induction stage and foaming stage. In the induction stage, the adverse chemical behaviors of activated OBSH were pre-eliminated. Activated OBSH via induction treatment released gas maximally and distributed gas homogeneously in the resin glue. The properties of the LDUPR with the activated OBSH via induction treatment were improved. The proposed induction treatment provided an innovation to the application of foaming agents without first-order reaction.

ACKNOWLEDGMENTS

The authors thank Jinling DSM Resins Co., for supplying materials; the foundation of the Priority Academic Program Development of Jiangsu Higher Education Institutions (PAPD 2011-6); and the Open Experimental Foundation of Nanjing University of Technology (2015DC007).

REFERENCES

1. Kocak, E. D. *J. Eng. Mater.-T. ASME* **2008**, *130*, 1.
2. Gao, Z. H.; Ma, D. Y.; Lv, X. Y.; Zhang, Y. H. *J. Appl. Polym. Sci.* **2013**, *128*, 1036.
3. Aruniit, A.; Kers, J.; Majak, J.; Krumme, A.; Tall, K. *Proc. Est. Acad. Sci.* **2012**, *61*, 160.
4. Guo, L. Z.; Wang, X. J.; Zhang, Y. F.; Wang, X. Y. *J. Appl. Polym. Sci.* **2014**, *131*, 40238.
5. Zhu, H. F.; Wang, X. J.; Guo, L. Z.; Zhang, Y. F. *Thermosetting Resin* **2013**, *34*, 28.
6. Zipfel, L.; Kruecke, W.; Boerner, K.; Barthelemy, P.; Dournel, P. *J. Cell. Plast.* **1998**, *34*, 511.
7. Barthelemy, P.; Zipfel, L. *Urethanes Technol.* **1997**, *14*, 36.
8. Klempner, D.; Frisch, K. C. Handbook of Polymeric Foams and Foam Technology; Hanser Publishers: Munich, **1991**.
9. Hunter, B. A.; Schoene, D. L. *Ind. Eng. Chem.* **1952**, *44*, 119.
10. Bayer, S. *Plast. Addit. Compos.* **2001**, *3*, 16.
11. Pop-Lliev, R.; Liu, F. Y.; Liu, G. B. *Adv. Polym. Sci.* **2003**, *22*, 280.
12. Sahin, E.; Machlicli, F. Y.; Yetgin, S.; Balkose, D. *J. Appl. Polym. Sci.* **2012**, *125*, 1448.
13. Li, G.; Qi, R. R.; Lu, J. Q. *J. Appl. Polym. Sci.* **2013**, *127*, 3586.
14. Petchwattana, N.; Covavisaruch, S.; Pitidhammabhorn, D. *J. Polym. Res.* **2013**, *20*, 172.
15. Petchwattana, N.; Covavisaruch, S. *Mater. Des.* **2011**, *32*, 2844.
16. Mao, Y. P.; Qi, R. R. *J. Appl. Polym. Sci.* **2008**, *109*, 3249.
17. Rowland, D. G. *Rubber Chem. Technol.* **1993**, *66*, 463.
18. Jeong, J.; Kim, T.; Cho, W. J.; Chung, I. *Polym. Int.* **2013**, *62*, 1094.
19. Wang, X.; Feng, N.; Chang, S. Q. *Polym. Compos.* **2013**, *34*, 849.
20. Potente, H.; Morizer, E.; Obermann, C. H. *Polym. Eng. Sci.* **1996**, *36*, 2163.
21. Amon, M.; Denson, C. D. *Polym. Eng. Sci.* **1986**, *26*, 255.
22. Arefmanesh, A.; Advani, S. G. *Polym. Eng. Sci.* **1995**, *35*, 252.
23. Talat-Erben, M.; Bywater, S. *J. Am. Chem. Soc.* **1955**, *77*, 3712.
24. Neiner, D.; Karkamkar, A.; Bowden, M.; Choi, Y. J.; Luedtke, A.; Holladay, J.; Fisher, A.; Szymczak, N.; Autrey, T. *Energy Environ. Sci.* **2011**, *10*, 4187.

25. Jeong, J.; Yang, J.; Ha, C. S.; Cho, W. J.; Chung, I. *Polym. Bull.* **2012**, *68*, 1227.
26. Ai, B.; Chen, L. L.; Li, J. L. *Chem Fert Ind.* **2010**, *37*, 18.
27. Arunan, E.; Desiraju, G. R.; Klein, R. A. *Pure Appl. Chem.* **2011**, *83*, 1637.
28. Tien, Y. I.; Wei, K. H. *Polymer* **2001**, *42*, 3213.
29. Qu, S. N.; Wang, H. T.; Bai, B. L. *Chem. Mater.* **2007**, *19*, 4839.
30. Bai, B. L.; Zhao, C. Y.; Wang, H. T. *Mater. Chem. Phys.* **2012**, *133*, 232.
31. Ran, X.; Wang, H. T.; Zhang, P. *Soft Matter* **2011**, *7*, 8561.
32. Zhao, X.; Wang, X. Z.; Jiang, X. K. *J. Am. Chem. Soc.* **2003**, *125*, 15128.
33. Lazic, V.; Jurkovic, M.; Jednacak, T. *J. Mol. Struct.* **2015**, *1079*, 243.
34. Zweifel, H.; Maier, R. D.; Schiller, M. Plastics Additives Handbook; Hanser Verlag: Munich, **2009**.
35. Chul, B. P.; John, J. B. *Polym. Eng. Sci.* **1998**, *11*, 1862.
36. Oertel, G. Polyurethane Handbook, 2nd ed.; Hanser Publishers: New York, **1994**.